

Efficiency large deviation function of quantum heat engines

Tobias Denzler and Eric Lutz

Institute for Theoretical Physics I, University of Stuttgart, D-70550 Stuttgart, Germany

The efficiency of small thermal machines is typically a fluctuating quantity. We here study the efficiency large deviation function of two exemplary quantum heat engines, the harmonic oscillator and the two-level Otto cycles. While the efficiency statistics follows the 'universal' theory of Verley *et al.* [Nature Commun. 5, 4721 (2014)] for nonadiabatic driving, we find that the latter framework does not apply in the adiabatic regime. We relate this unusual property to the perfect anticorrelation between work output and heat input that generically occurs in the broad class of scale-invariant adiabatic quantum Otto heat engines and suppresses thermal as well as quantum fluctuations.

Fluctuations play a central role in the thermodynamics of small systems. Contrary to macroscopic thermodynamics that describes the average behavior of a vast number of particles, microscopic systems are characterized by stochastic variables, whose large fluctuations from mean values contain useful information on their dynamics [1]. At equilibrium, the probability distributions of thermal observables are conveniently obtained using the methods of equilibrium statistical physics [2]. However, their evaluation for nonequilibrium problems is often difficult. A powerful framework that allows the calculation of these distributions, both in equilibrium and nonequilibrium situations, is provided by large deviation theory [3–6]. From a physical point of view, the large deviation approach may be viewed as a generalization of the Einstein theory of fluctuations that relates the probability distribution to the entropy, $P(x) \sim \exp[S(x)/k]$, where k is the Boltzmann constant. On the other hand, from a mathematical standpoint, it may be regarded as an extension of the law of large numbers and the central-limit theorem [3–6].

Large deviation techniques have found widespread application in many areas, ranging from Brownian motion and hydrodynamics to disordered and chaotic systems [3–6]. In the past few years, they have been successfully employed to investigate the efficiency statistics of small thermal machines [7–21]. In microscopic systems, heat, work, and, consequently, efficiency are indeed random quantities owing to the presence of thermal [1] and, at low enough temperatures, quantum fluctuations [22, 23]. Understanding their fluctuating properties is therefore essential. In particular, Refs. [7, 8] have identified 'universal' features of the efficiency large deviation function, which exhibits a characteristic smooth form with two extrema, including a maximum at the Carnot efficiency. The latter value is thus remarkably the least likely in the long-time limit. These predictions have been experimentally verified for a stochastic harmonic heat engine based on an optically trapped colloidal particle [24].

In this paper, we compute the efficiency large deviation function of two paradigmatic quantum thermal machines, the harmonic oscillator quantum engine and the two-level system quantum motor [25–36]. Our study is motivated by the recent experimental implementation of a nanoscopic harmonic heat engine using a single trapped ion [37] and the realization of quantum spin-1/2 motors

using NMR [38, 39] and trapped ion [40] setups. We concretely consider the exemplary case of the quantum Otto cycle, a generalization of the ordinary four-stroke motor that has been extensively studied in the past thirty years [41]. We find that the efficiency large deviation functions follow the 'universal' form of Refs. [7, 8] for nonadiabatic driving. However, in the adiabatic regime, which corresponds to maximum efficiency and may be reached exactly for a periodically driven two-level engine or using shortcut-to-adiabaticity techniques [42–44], we show that the large deviation functions take a markedly different shape, as the efficiency is deterministic and equal to the macroscopic Otto efficiency. This result holds generically for heat engines with scale-invariant Hamiltonians that describe a broad class of single-particle, many-body and nonlinear systems [45–49]. We trace this unusual behavior to the perfect anticorrelation between work output and heat input within the engine cycle that is established for adiabatic driving. This property completely suppresses the effects of fluctuations. As a consequence, microscopic adiabatic quantum Otto heat engines run at the nonfluctuating macroscopic efficiency.

Efficiency large deviation function. We consider a generic quantum system with a time-dependent Hamiltonian H_t as the working medium of a quantum Otto engine. The engine is alternately coupled to two heat baths at inverse temperatures $\beta_i = 1/(kT_i)$, ($i = c, h$), where k is the Boltzmann constant. The quantum Otto cycle consists of the following four consecutive steps [41]: (1) Unitary expansion: the Hamiltonian is changed from H_0 to H_{τ_1} in a time τ_1 , consuming an amount of work W_1 , (2) Hot isochore: the system is weakly coupled to the hot bath at inverse temperature β_h to absorb heat Q_2 in a time τ_2 , (3) Unitary compression: the isolated system is driven from H_{τ_1} back to H_0 in a time τ_3 , producing an amount of work W_3 , and (4) Cold isochore: the cycle is closed by connecting the system to the cold bath at inverse temperature β_c , releasing heat Q_4 in a time τ_4 . Work and heat are positive, when added to the system. We further assume that heating and cooling times, $\tau_{2,4}$, are longer than the relaxation time, so that the system can fully thermalize after each isochore, as in the experimental quantum Otto engines of Refs. [38, 39]. Without loss of generality, we additionally set $\tau_1 = \tau_3 = \tau$.

The stochastic efficiency of the microscopic quantum

heat engine is defined as the ratio of work output and heat input, $\eta = -W/Q_2$, where $W = W_1 + W_3$ denotes the total work [7–21]. It should not be confused with the thermodynamic efficiency of macroscopic engines, $\eta_{\text{th}} = -\langle W \rangle / \langle Q_2 \rangle$, which is given by the ratio of the mean work output and the mean heat input, and is thus a deterministic quantity. We investigate the efficiency statistics of the quantum engine in the long-time limit using large deviation theory [3–6]. Following Refs. [7, 8], we write the joint distribution of work and heat, $P_s(Q_2, W)$, as well as the efficiency distribution $P_s(\eta)$, for a large number of cycles ($s \gg 1$), in the asymptotic form,

$$P_s(Q_2, W) \approx e^{-sI(Q_2, W)} \quad \text{and} \quad P_s(\eta) \approx e^{-sJ(\eta)}. \quad (1)$$

The two large deviation functions $I(Q_2, W)$ and $J(\eta)$ describe the exponentially unlikely deviations of the variables Q_2 , W and η from their typical values. The rate function $J(\eta)$ follows from $I(Q_2, W)$ by contraction [6],

$$J(\eta) = \min_{Q_2} I(Q_2, -\eta Q_2). \quad (2)$$

An alternative, more practical, expression may be obtained by introducing the bivariate scaled cumulant generating function of the mean heat and mean work per cycle, $q_2^{(s)} = \sum_{j=1}^s Q_2^{(j)} / s$ and $w^{(s)} = \sum_{j=1}^s W^{(j)} / s$ [8]:

$$\begin{aligned} \phi(\gamma_1, \gamma_2) &= \lim_{s \rightarrow \infty} \frac{1}{s} \ln \langle e^{s(\gamma_1 q_2^{(s)} + \gamma_2 w^{(s)})} \rangle \\ &= \ln \langle e^{\gamma_1 Q_2 + \gamma_2 W} \rangle. \end{aligned} \quad (3)$$

Using the Legendre-Fenchel transform, one then finds [8],

$$J(\eta) = -\min_{\gamma_2} \phi(\gamma_2 \eta, \gamma_2). \quad (4)$$

The efficiency large deviation function $J(\eta)$ may thus be determined from the scaled cumulant generating function $\phi(\gamma_1, \gamma_2)$. In the following, we evaluate $\phi(\gamma_1, \gamma_2)$ by taking the logarithm of the moment generating function, that is, the Wick transformed characteristic function $G(\gamma_1, \gamma_2) = \langle \exp(-i\gamma_1 Q_2 - i\gamma_2 W) \rangle$ [51].

Work-heat correlations. Work output and heat input are usually correlated in a closed quantum heat engine cycle. Despite their fundamental importance, their correlations have received little attention so far [52]. We next derive their joint probability distribution using the standard two-projective-measurement approach [53]. In this method, energy changes of a quantum system during single realizations of a process are identified with the difference of energy eigenvalues obtained through projective measurements at the beginning and at the end of the process. In the quantum Otto cycle, work is performed during the unitary expansion and compression stages, while heat is exchanged during the nonunitary heating and cooling steps. We obtain the distributions of work and heat by applying the two-projective-measurement scheme to the respective expansion, hot isochore and compression branches. The corresponding joint distribution for

work output and heat input reads accordingly [54],

$$\begin{aligned} P(Q_2, W) &= \sum_{n,m,k,l} \delta [W - (E_m^\tau - E_n^0 + E_l^0 - E_k^\tau)] \\ &\times \delta [Q_2 - (E_k^\tau - E_m^\tau)] P_n^0(\beta_c) P_k^\tau(\beta_h) \\ &\times |\langle n | U_{\text{exp}}(\tau) | m \rangle|^2 |\langle k | U_{\text{com}}(\tau) | l \rangle|^2, \end{aligned} \quad (5)$$

where E_n^0 (E_k^τ) and E_m^τ (E_l^0) are the respective energy eigenvalues at the beginning and at the end of the expansion (compression) step, with corresponding unitary operator U_{exp} (U_{com}). The thermal distribution at the beginning of the expansion (compression) stage is given by $P_n^0(\beta_c) = \exp(-\beta_c E_n^0) / Z_0$ ($P_k^\tau(\beta_h) = \exp(-\beta_h E_k^\tau) / Z_\tau$). The occupation probabilities $P_n^0(\beta_c)$ and $P_k^\tau(\beta_h)$ account for thermal fluctuations, while the transition probabilities $|\langle n | U_{\text{exp}}(\tau) | m \rangle|^2$ and $|\langle k | U_{\text{com}}(\tau) | l \rangle|^2$ for both quantum fluctuations and quantum dynamics [50].

We study the generic features of work-heat correlations in the adiabatic regime by considering scale-invariant Hamiltonians of the form $H_\tau = \mathbf{p}^2 / 2m + U(\mathbf{x}, \varepsilon_\tau)$ with $U(\mathbf{x}, \varepsilon_\tau) = U_0(\mathbf{x} / \varepsilon_\tau) / \varepsilon_\tau^2$ and scaling parameter ε_τ . Such Hamiltonians describe a large class of single-particle, many-body and nonlinear systems with scale-invariant spectra, $E_j^\tau = E_j^0 / \varepsilon_\tau^2$ [45–49]. Taking the Fourier transform of Eq. (5), we obtain the characteristic function,

$$\begin{aligned} G(\gamma_1, \gamma_2) &= \frac{1}{Z_0 Z_\tau} \sum_n e^{[-\beta_c + i\varepsilon_\tau^{-2} \gamma_1 + i(1 - \varepsilon_\tau^{-2}) \gamma_2] E_n^0} \\ &\times \sum_k e^{[-\beta_h \varepsilon_\tau^{-2} - i\varepsilon_\tau^{-2} \gamma_1 - i(1 - \varepsilon_\tau^{-2}) \gamma_2] E_k^\tau}, \end{aligned} \quad (6)$$

with the transition probabilities $|\langle m | U_{\text{exp}} | n \rangle|^2 = \delta_{nm}$ and $|\langle k | U_{\text{com}} | l \rangle|^2 = \delta_{kl}$ for adiabatic expansion and compression. Remarkably, Eq. (6) is constant along straight lines with a slope given by the macroscopic efficiency $\eta_{\text{th}} = 1 - \varepsilon_\tau^2$. We specifically have $G(\gamma_1, \gamma_2) = G(\gamma_1^0, \gamma_2^0)$ for $\gamma_1 = \eta_{\text{th}}(\gamma_2 - \gamma_2^0) + \gamma_1^0$. This result has profound implications for the work-heat correlations and the large deviation properties of the quantum engine.

We first remark that work output and heat input are perfectly anticorrelated in this case, with a Pearson coefficient [55], $\rho = \text{cov}(Q_2, W) / \sigma_{Q_2} \sigma_W = -1$ (Fig. 1) [54]. On the other hand, the minimization in Eq. (4) leads to a rate function that plateaus at infinity, except at the macroscopic efficiency η_{th} where it vanishes (Fig. 2). As a consequence, the microscopic stochastic efficiency is deterministic and equal to the macroscopic value η_{th} . Adiabatic quantum Otto engines hence lie outside the universality class of Refs. [7, 8]. This may be understood by noting that quantum work fluctuations are suppressed in the adiabatic regime. Thermal fluctuations are additionally canceled by the perfect work-heat anticorrelation.

Quantum heat engines. Let us now examine the work-heat correlations and the efficiency large deviations, both in the adiabatic and nonadiabatic regimes, for two exactly solvable quantum Otto engines. We first evaluate the characteristic function $G(\gamma_1, \gamma_2)$ for a solvable two-level quantum motor. Inspired by the recent NMR ex-

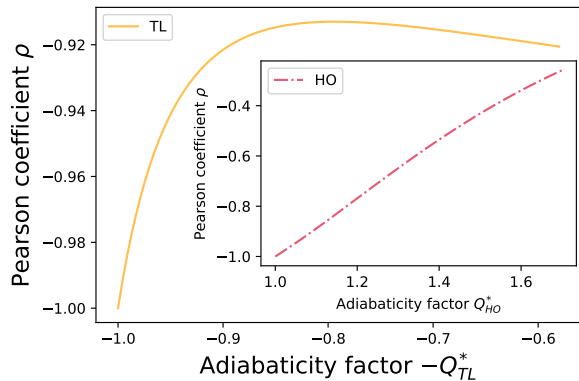


FIG. 1. Work-heat Pearson coefficient in a harmonic (red dotted-dashed) and two-level (orange solid) Otto cycle. Work output and heat input are anticorrelated with perfect adiabatic anticorrelation, $\rho = -1$ for $Q_{\text{HO}}^* = Q_{\text{TL}}^* = 1$. Parameters are $\omega_0 = \nu_0 = 1$, $\omega_\tau = \nu_\tau = 2$, $\beta_c = 3$ and $\beta_h = 0.1$.

periments [38, 39], we consider the expansion Hamiltonian, $H_t^{\text{exp}} = \omega \sigma_z / 2 + \lambda(t) (\cos \omega t \sigma_x + \sin \omega t \sigma_y)$, that describes a spin-1/2 driven by a constant magnetic field with strength $\omega/2$ along the z -axis and a rotating magnetic field with varying strength $\lambda(t)$ in the $(x-y)$ -plane, where σ_i , $i = (x, y, z)$, are the standard Pauli operators (with $\hbar = 1$). The rotation frequency is chosen to be $\omega = \pi/2\tau$ to ensure a complete rotation from the x -axis to the y -axis during time τ . The amplitude of the rotating field, $\lambda(t) = \lambda_1 (1 - t/\tau) + \lambda_2 (t/\tau)$, is increased from λ_1 at time zero to λ_2 at time τ . This driving leads to a widening of the energy spacing of the two-level system from $2\nu_0 = \sqrt{4\lambda(0)^2 + \omega^2}$ to $2\nu_\tau = \sqrt{4\lambda(\tau)^2 + \omega^2}$. The compression Hamiltonian is obtained from the time reversed process, $H_t^{\text{com}} = -H_{\tau-t}^{\text{exp}}$. The characteristic function $G(\gamma_1, \gamma_2)$ may be determined by solving the time evolution of the engine. It is explicitly given by [54],

$$G_{\text{TL}}(\gamma_1, \gamma_2) = \frac{1}{Z_0 Z_\tau} \left\{ 2 \cosh(x+y) u^2 + 2 \cosh(x-y) v^2 + 2 u v e^{-x} \cosh(y) e^{-i2\omega_0 \gamma_2} + 2 u v e^x \cosh(y) e^{i2\omega_0 \gamma_2} + u^2 e^{x-y} e^{i2\omega_\tau \gamma_1} e^{i2(\omega_0 - \omega_\tau) \gamma_2} + v^2 e^{-x-y} e^{i2\omega_\tau \gamma_1} e^{-i2(\omega_0 + \omega_\tau) \gamma_2} + 2 u v e^{-y} \cosh(x) e^{i2\omega_\tau \gamma_1} e^{-i2\omega_\tau \gamma_2} + u^2 e^{-x+y} e^{-i2\omega_\tau \gamma_1} e^{i2(\omega_\tau - \omega_0) \gamma_2} + v^2 e^{x+y} e^{-i2\omega_\tau \gamma_1} e^{i2(\omega_0 + \omega_\tau) \gamma_2} + 2 u v e^y \cosh(x) e^{-i2\omega_\tau \gamma_1} e^{i2\omega_\tau \gamma_2} \right\}. \quad (7)$$

where $u = 1 - v$ denotes the probability of no-level transition ($0 \leq u \leq 1$), $x = \beta_c \nu_0$ and $y = \beta_h \nu_\tau$ [54]. The two-level engine operates adiabatically, when the adiabaticity parameter, defined as the ratio of the nonadiabatic and adiabatic mean energies, $Q_{\text{TL}}^* = 2u - 1 = 1$ (or $u = 1$). We emphasize that, since the driving is periodic, the adiabatic regime is here reached exactly for $\int_0^\tau dt' \lambda(t') = n\pi$,

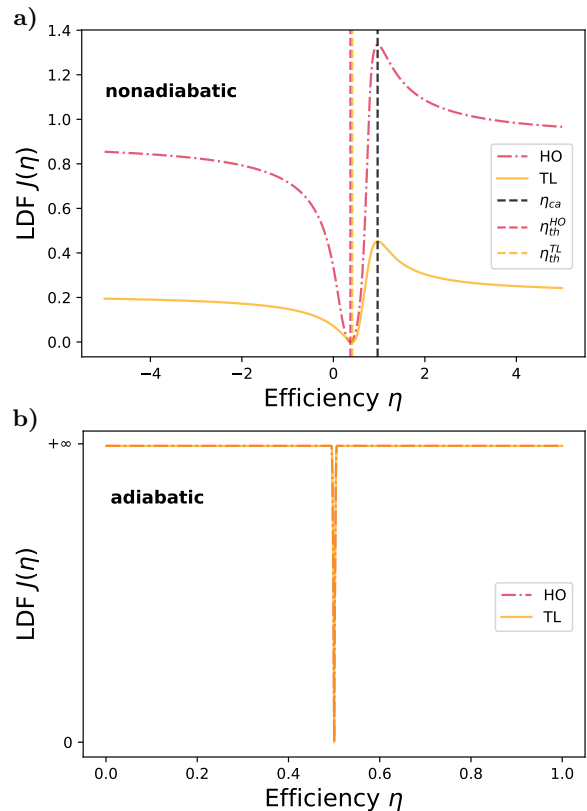


FIG. 2. Efficiency large deviation function (LDF). a) For nonadiabatic driving ($Q_{\text{HO}}^* = 1.2$, $Q_{\text{TL}}^* = 0.9$), $J(\eta)$ has the typical form of Refs. [7, 8] for both engines, with a maximum at the Carnot efficiency η_{ca} and a minimum at the macroscopic efficiency η_{th} . b) For adiabatic driving ($Q_{\text{HO}}^* = Q_{\text{TL}}^* = 1$), the efficiency is deterministic and $J(\eta)$ is infinite everywhere except at $\eta = \eta_{th}$. Same parameters as in Fig. 1.

and not just asymptotically for large driving times [54]. Equation (7) contains all the information needed to investigate the work-heat correlations and the efficiency large deviation function of the quantum two-level heat engine.

We next consider a (unit mass) harmonic oscillator engine with expansion Hamiltonian $H_t^{\text{exp}} = p^2/2 + \omega_t^2 x^2/2$, where ω_t the time-dependent frequency that is varied from ω_0 to ω_τ in time τ according to $\omega_t^2 = (1 - t/\tau) \omega_0^2 + \omega_\tau^2 t/\tau$. The reversed compression protocol is again obtained with the replacement $t = \tau - t$. This quantum Otto engine model is analytically solvable [34] and we find the work-heat characteristic function [54],

$$G_{\text{HO}}(\gamma_1, \gamma_2) = \frac{2}{Z_0 Z_\tau} \times \frac{1}{\sqrt{Q_{\text{HO}}^* (1 - u_0^2)(1 - v_0^2) + (1 + u_0^2)(1 + v_0^2) - 4u_0v_0}} \times \frac{1}{\sqrt{Q_{\text{HO}}^* (1 - x_0^2)(1 - y_0^2) + (1 + x_0^2)(1 + y_0^2) - 4x_0y_0}}, \quad (8)$$

where we have again introduced the adiabaticity parameter Q_{HO}^* , which is equal to 1 for adiabatic driving

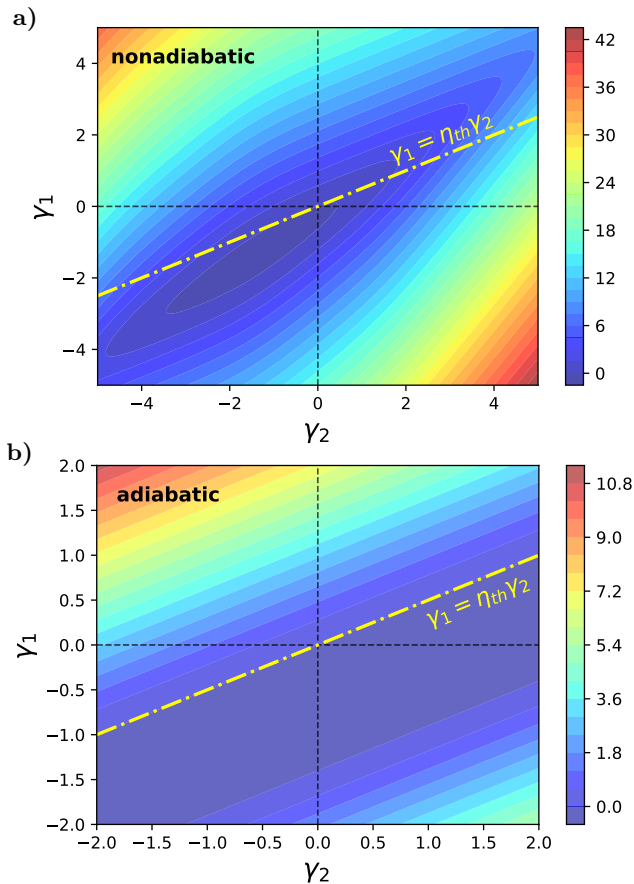


FIG. 3. Contour plot of the scaled cumulant generating function $\phi(\gamma_1, \gamma_2)$ for the two-level engine. a) In the nonadiabatic regime, the minimization along the line $\gamma_1 = \eta_{th} \gamma_2$ yields a unique solution, leading to the ‘universal’ LDF in Fig. 2a. b) In the adiabatic regime, the minimum is degenerate since the isocontours are parallel lines with slope η_{th} , resulting in the LDF in Fig. 2b. Same parameters as in Fig. 2.

[56, 57], as well as the variables $u_0 = \exp[-\omega_0(\beta_c + i\gamma_2)]$, $v_0 = \exp[i\omega_\tau(\gamma_2 - \gamma_1)]$, $x_0 = \exp[-\beta_h \omega_\tau + i\omega_\tau(\gamma_1 - \gamma_2)]$ and $y_0 = \exp(i\gamma_2 \omega_0)$ [54]. The work-heat correlation and the efficiency large deviations of the harmonic oscillator heat engine may be examined with the help of Eq. (8).

Results. We begin by analyzing the work-heat correlations within the quantum Otto cycle using the Pearson coefficient. Figure 1 shows the correlation coefficient ρ for the qubit (orange solid) and the harmonic (red dotted-dashed) quantum heat engines as a function of the respective adiabaticity parameters (we have set their frequencies equal, $\omega_j = \nu_j$, in order to compare the two cases). We observe that work output and heat input are generally negatively correlated in both examples. However, contrary to the harmonic engine, the two-level motor displays a nonmonotonous dependence on Q^* due to the finite dimension of its Hilbert space. We, moreover, see that the amount of correlations increases with decreasing nonadiabaticity. In particular, work output

and heat input are perfectly anticorrelated for adiabatic cycles, in agreement with the result obtained for scale-invariant engines.

Figure 2 exhibits the large deviation function $J(\eta)$ for both working media. For nonadiabatic driving (Fig. 2a), we recognize the characteristic form obtained in Refs. [7, 8], with a maximum at the Carnot efficiency η_{ca} (the least likely value) and a minimum located at the macroscopic Otto efficiency η_{th} (the most likely value). The harmonic rate function is, furthermore, strictly above that of the qubit (with the exception of the root at η_{th}), indicating that the harmonic heat engine converges faster towards the macroscopic efficiency η_{th} than the two-level engine. By contrast, for adiabatic driving (Fig. 2b), when work output and heat input are perfectly anticorrelated, the rate function of both systems noticeably departs from that general form: it is zero at the thermodynamic efficiency η_{th} and infinite everywhere else, confirming that the efficiency behaves deterministically. It is important to stress that these findings are not restricted to the strict adiabatic limit [54]. They are also valid in the linear response regime, which is often used to examine the finite-time dynamics of quantum heat engines [58–60].

A deeper understanding of the stark differences between adiabatic and nonadiabatic driving in the quantum Otto cycle may be gained by applying the geometric approach of Ref. [20] to the present instance of quantum heat engines. According to Eq. (4), the rate function $J(\eta)$ is obtained for fixed η by minimizing the cumulant generating function $\phi(\gamma_1, \gamma_2)$ along the line $\gamma_1 = \eta \gamma_2$. The theory of Refs. [7, 8] then only applies when there is a unique minimum. This is the case for nonadiabatic driving, as can be seen from the contour plot of $\phi(\gamma_1, \gamma_2)$ for the two-level quantum motor (Fig. 3a). By contrast, for adiabatic driving, the isocontours of $\phi(\gamma_1, \gamma_2)$ are parallel lines with slope η_{th} (Fig. 3b). As a result, the minimum is degenerate, leading to the plateau of the large deviation function at infinity (except at the macroscopic efficiency η_{th}) and the breakdown of the formalism of Refs. [7, 8]. A similar behavior is observed for the example of the harmonic quantum heat engine [54].

Conclusions. We have investigated the work-heat correlations and the efficiency statistics of the quantum Otto cycle with a working medium consisting of a two-level system or a harmonic oscillator. We have found that work output and heat input are in general negatively correlated, with perfect anticorrelation achieved for adiabatic driving. As a consequence, the microscopic quantum efficiency is equal to the deterministic macroscopic Otto efficiency and the efficiency large deviation function strongly deviates from the characteristic form obtained in Refs. [7, 8]. These results not only hold for quantum heat engines that operate in the adiabatic limit, such as shortcut-to-adiabaticity engines, but also in the linear response regime. Our findings are thus important for the study of the performance of small quantum thermal machines that run close to the adiabatic regime.

We acknowledge financial support from the German

Science Foundation (DFG) under project FOR 2724.

SUPPLEMENTAL MATERIAL

I. WORK-HEAT CORRELATIONS

We here derive the joint probability distribution of work output and heat input $P(Q_2, W)$, Eq. (5) in the main text, using the two-projective-measurement scheme [53]. Performing a projective energy measurement at the beginning and at end of the expansion step, we obtain the expansion work distribution $P(W_1)$,

$$P(W_1) = \sum_{n,m} \delta [W_1 - (E_m^\tau - E_n^0)] P_{n \rightarrow m}^\tau P_n^0(\beta_c), \quad (9)$$

where E_n^0 and E_m^τ are the respective energy eigenvalues, $P_n^0(\beta_c) = \exp(-\beta_c E_n^0)/Z_0$ is the initial thermal occupation probability and $P_{n \rightarrow m}^\tau = |\langle n | U_{\text{exp}} | m \rangle|^2$ the transition probability between the instantaneous eigenstates $|n\rangle$ and $|m\rangle$. The corresponding unitary is denoted by U_{exp} . Similarly, the probability density of the heat Q_2 during the following hot isochore, given the expansion work W_1 , is equal to the conditional distribution [61],

$$P(Q_2|W_1) = \sum_{k,l} \delta [Q_2 - (E_l^\tau - E_k^\tau)] P_{k \rightarrow l}^{\tau_2} P_k^\tau, \quad (10)$$

where the occupation probability at time τ is $P_k^\tau = \delta_{km}$ when the system is in eigenstate $|m\rangle$ after the second projective energy measurement during the expansion step. Noting that the state of the system is thermal with inverse temperature β_h at the end of the isochore, we further have $P_{k \rightarrow l}^{\tau_2} = P_l^{\tau_2}(\beta_h) = \exp(-\beta_h E_l^\tau)/Z_\tau$. The quantum work distribution for compression, given the expansion work W_1 and the heat Q_2 , is moreover,

$$P(W_3|W_1, Q_2) = \sum_{i,j} \delta [W_3 - (E_j^0 - E_i^\tau)] P_{i \rightarrow j}^\tau P_i^{\tau+\tau_2}, \quad (11)$$

with the occupation probability $P_i^{\tau+\tau_2} = \delta_{il}$ when the system is in eigenstate $|l\rangle$ after the third projective energy measurement. The transition probability $P_{i \rightarrow j}^\tau = |\langle i | U_{\text{com}} | j \rangle|^2$ is fully specified by the unitary time evolution operator for compression U_{com} .

The joint probability of having certain values of W_3 , Q_2 and W_1 during the cycle follows from the chain rule for conditional probabilities, $P(W_3, Q_2, W_1) = P(W_3|Q_2, W_1)P(Q_2|W_1)P(W_1)$ [51]. We find [62],

$$\begin{aligned} P(W_1, Q_2, W_3) &= \sum_{n,m,k,l} \delta [W_1 - (E_m^\tau - E_n^0)] \\ &\times \delta [Q_2 - (E_k^\tau - E_m^\tau)] \delta [W_3 - (E_l^0 - E_k^\tau)] \\ &\times |\langle n | U_{\text{exp}} | m \rangle|^2 |\langle k | U_{\text{com}} | l \rangle|^2 \\ &\times \frac{e^{-\beta_c E_n^0} e^{-\beta_h E_k^\tau}}{Z_0 Z_\tau}. \end{aligned} \quad (12)$$

The joint distribution $P(Q_2, W)$ then follows by integrating over the work contributions W_1 and W_2 , $P(Q_2, W) = \int dW_1 dW_3 \delta [W - (W_1 + W_3)] P(W_1, Q_2, W_3)$.

We next compute the characteristic function, Eq. (6) of the main text, and the Pearson coefficient for adiabatic scale invariant quantum Otto heat engines with Hamiltonian $H_t = \mathbf{p}^2/2m + U(\mathbf{x}, \varepsilon_\tau)$ with $U(\mathbf{x}, \varepsilon_\tau) = U_0(\mathbf{x}/\varepsilon_\tau)/\varepsilon_\tau^2$. In the adiabatic regime, $|\langle m | U_{\text{exp}} | n \rangle|^2 = \delta_{nm}$ and $|\langle k | U_{\text{com}} | l \rangle|^2 = \delta_{kl}$, we have,

$$\begin{aligned} P_{\text{ad}}(Q_2, W) &= \sum_{n,k} \delta [W - (1 - \varepsilon_\tau^{-2}) (E_k^0 - E_n^0)] \\ &\times \delta [Q_2 - (E_k^0 - E_n^0) \varepsilon_\tau^{-2}] \\ &\times \frac{e^{-\beta_c E_n^0 - \beta_h E_k^0 / \varepsilon_\tau^2}}{Z_0 Z_\tau}. \end{aligned} \quad (13)$$

The characteristic function $G(\gamma_1, \gamma_2) = \langle \exp(-i\gamma_1 Q_2 - i\gamma_2 W) \rangle$, Eq. (6) of the main text, is readily obtained after Fourier transformation.

The Pearson coefficient in this case follows as,

$$\begin{aligned} \rho &= \frac{\text{cov}(Q_2, W)}{\sigma_{Q_2} \sigma_W} \\ &= \frac{\langle Q_2 W \rangle - \langle Q_2 \rangle \langle W \rangle}{(\langle Q_2^2 \rangle - \langle Q_2 \rangle^2)(\langle W^2 \rangle - \langle W \rangle^2)} \\ &= \frac{(1 - \varepsilon_\tau^{-2})}{|(1 - \varepsilon_\tau^{-2})|} = \pm 1. \end{aligned} \quad (14)$$

We observe that work-heat correlations are always maximal in the adiabatic regime. By further considering the heat engine conditions,

$$\langle Q_2 \rangle = \varepsilon_\tau^{-2} \sum_{n \neq k} \frac{e^{-\beta_c E_n^0 - \beta_h E_k^0 / \varepsilon_\tau^2}}{Z_0 Z_\tau} (E_k^0 - E_n^0) \geq 0 \quad (15)$$

$$\langle W \rangle = (1 - \varepsilon_\tau^{-2}) \sum_{n \neq k} \frac{e^{-\beta_c E_n^0 - \beta_h E_k^0 / \varepsilon_\tau^2}}{Z_0 Z_\tau} (E_k^0 - E_n^0) \leq 0,$$

we find that $(1 - \varepsilon_\tau^{-2}) \leq 0$. As a result, work output and heat input are perfectly anticorrelated for an adiabatic quantum Otto engine, $\rho = -1$. We can thus conclude that, even though the engine is still subjected to non-vanishing heat and work fluctuations, they fluctuate in unison such that its efficiency is deterministic.

II. CHARACTERISTIC FUNCTIONS

We next evaluate the characteristic function $G_{\text{TL}}(\gamma_1, \gamma_2)$, Eq. (7) of the main text, for the exactly solvable two-level quantum Otto engine. The time evolution operator U_{exp} for the expansion branch may be calculated using the methods of Refs. [62–64],

$$U_{\text{exp}} = \begin{pmatrix} e^{-i\omega t/2} \cos I & i e^{-i\omega t/2} \sin I \\ i e^{i\omega t/2} \sin I & e^{i\omega t/2} \cos I \end{pmatrix}, \quad (16)$$

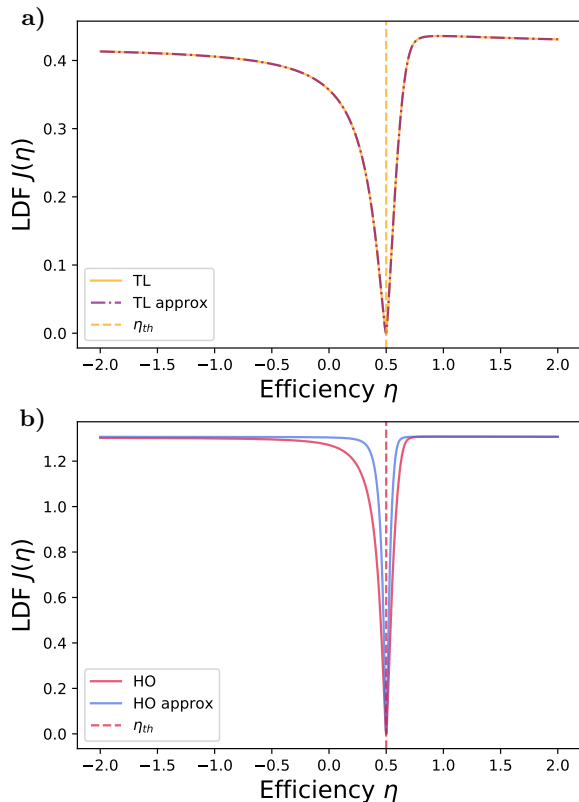


FIG. 4. Efficiency large deviation function (LDF) in the linear response regime. a) Exact $J(\eta)$ for the two-level quantum engine (orange solid) and linear approximation (purple dotted-dashed) for $Q_{\text{TL}}^* = 0.998$. b) Exact $J(\eta)$ for the harmonic heat engine (red solid) and linear approximation (blue dotted) for $Q_{\text{HO}}^* = 1.0005$. In both cases, the maximum at the Carnot efficiency η_{ca} effectively disappears and the peak at the macroscopic efficiency η_{th} is broadened. Same parameters as in Fig. 1 of the main text.

where $I = -\int_0^t dt' \lambda(t')$ is the integral over the increasing strength of the rotating magnetic field. The operator U_{com} follows from U_{exp} by the replacement t with $\tau - t$. The probability of no level transition during expansion or compression are identical for $\tau_1 = \tau_3 = \tau$ and reads,

$$\begin{aligned} u &= u_{\text{exp}} = |\langle 0|U_{\text{exp}}|0\rangle| = |\langle 1|U_{\text{exp}}|1\rangle| = \cos^2 I, \\ &= u_{\text{com}} = |\langle 0|U_{\text{com}}|0\rangle| = |\langle 1|U_{\text{com}}|1\rangle|. \end{aligned} \quad (17)$$

The probability of a (nonadiabatic) level transition during either driving phases is accordingly $v = 1 - u$. The adiabaticity parameter is defined as the ratio $Q_{\text{TL}}^* = \langle H_\tau \rangle_{\text{nad}} / \langle H_\tau \rangle_{\text{ad}} = 2u - 1$ [49] and is equal to 1 for adiabatic driving, $u = 1$. Inserting the above expressions for the transition probabilities into $P(Q_2, W)$ and performing the Fourier transform, $\iint dW dQ_2 \exp(-i\gamma_1 Q_2 - i\gamma_2 W) P(Q_2, W)$, then yields the characteristic function $G_{\text{TL}}(\gamma_1, \gamma_2)$.

The characteristic function $G_{\text{HO}}(\gamma_1, \gamma_2)$, Eq. (8) of the main text, for the exactly solvable harmonic quantum Otto engine may be directly evaluated using a result of

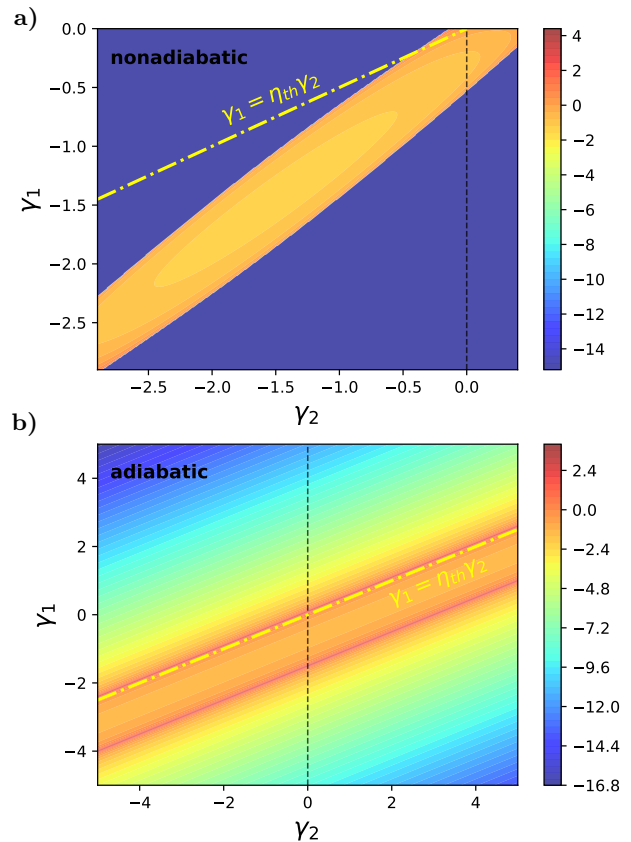


FIG. 5. Contour plot of the scaled cumulant generating function $\phi(\gamma_1, \gamma_2)$ for the harmonic quantum engine. a) In the nonadiabatic regime ($Q_{\text{HO}}^* = 1.2$), the minimization along the line $\gamma_1 = \eta_{\text{th}} \gamma_2$ yields a unique solution. b) In the adiabatic regime ($Q_{\text{HO}}^* = 1$), the minimum is degenerate since the isocontours are parallel lines with slope η_{th} .

Ref. [57]. The generating function of the transition probabilities for expansion is indeed given by,

$$\begin{aligned} P(u', v') &= \sum_{n,m} u_0^n v_0^m P_{n \rightarrow m}^\tau \\ &= \frac{\sqrt{2}}{\sqrt{Q_{\text{HO}}^* (1 - u_0^2)(1 - v_0^2) + (1 + u_0^2)(1 + v_0^2) - 4u_0 v_0}}. \end{aligned} \quad (18)$$

and a similar expression for the compression step. We then determine the characteristic function $G_{\text{HO}}(\gamma_1, \gamma_2)$ by comparing the terms of different powers in (n, m, k, l) of the Fourier transform of Eq. (5) of the main text with the ones in Eq. (18).

III. LINEAR-RESPONSE REGIME

The performance of (nonadiabatic) finite-time quantum heat engines is often analyzed in the linear response regime, that is, in a first-order expansion around the adiabatic limit [58–60]. We show in this section that the

large deviation function $J(\eta)$ still deviates from the general form of Refs. [7, 8]. For the two-level Otto engine, a Taylor expansion in first-order around $u = 1$ yields the work-heat characteristic function,

$$\begin{aligned}
G_{\text{TL}}^{\text{lin}}(\gamma_1, \gamma_2) = & \frac{1}{Z_0 Z_\tau} \left\{ e^{2i\gamma_2(\omega_0 - \omega_\tau) + 2i\gamma_1\omega_\tau + x - y} \right. \\
& + e^{-2i\gamma_1\omega_\tau + 2i\gamma_2(\omega_\tau - \omega_0) - x + y} + 2 \cosh(x + y) \\
& + 2(u - 1) \left[e^{2i\gamma_2(\omega_0 - \omega_\tau) + 2i\gamma_1\omega_\tau + x - y} \right. \\
& + e^{-2i\gamma_1\omega_\tau + 2i\gamma_2(\omega_\tau - \omega_0) - x + y} \\
& - \cosh(x) e^{2i\gamma_1\omega_\tau - 2i\gamma_2\omega_\tau - y} \\
& - \cosh(x) e^{-2i\gamma_1\omega_\tau + 2i\gamma_2\omega_\tau + y} \\
& - \cosh(y) e^{-x - 2i\gamma_2\omega_0} - \cosh(y) e^{x + 2i\gamma_2\omega_0} \\
& \left. \left. + 4 \cosh(x + y) \right] \right\}. \tag{19}
\end{aligned}$$

where the parameters x, y, u, v are unchanged.

On the other hand, a Taylor expansion in first-order around $Q_{\text{HO}}^* = 1$ yields the work-heat characteristic function for the harmonic quantum Otto heat engine,

$$\begin{aligned}
G_{\text{HO}}^{\text{lin}}(\gamma_1, \gamma_2) = & \frac{1}{Z_0 Z_\tau} \left\{ \frac{1}{(1 - u_0 v_0)(1 - x_0 y_0)} \right. \\
& + \frac{1 - q}{4(1 - u_0 v_0)^3 (1 - x_0 y_0)^3} \\
& \times [(1 - x_0^2)(1 - y_0^2)(1 - u_0 v_0)^2 \\
& \left. + (1 - u_0^2)(1 - v_0^2)(1 - x_0 y_0)^2] \right\}, \tag{20}
\end{aligned}$$

where the parameters x_0, y_0, u_0, v_0 are also unchanged.

The corresponding approximate and exact large deviation functions $J(\eta)$ are shown in Fig. 4a) for the two-level engine and in Fig. 4b) for the harmonic motor. We observe in both cases that the maximum at the Carnot efficiency η_{ca} has effectively disappeared and that the narrow peak at the minimum located at the macroscopic efficiency η_{th} has instead broadened.

IV. HARMONIC SCALED CUMULANT GENERATING FUNCTION

We finally show the contour plots of the scaled cumulant generating function $\phi(\gamma_1, \gamma_2)$ of the harmonic quantum Otto engine in the nonadiabatic (Fig. 5a) and adiabatic (Fig. 5b) regimes. They are qualitatively similar to those of the two-level quantum motor represented in Fig. 3 of the main text. In the nonadiabatic case, we find regions in the (γ_1, γ_2) -plane for which the cumulant generating function is undefined (dark blue), contrary to what happens for the two-level Otto engine. This might lead to additional deviations from the 'universal' theory of Refs. [7, 8] as those already pointed out in Ref. [20]. In the adiabatic case, we again observe parallel lines with slope η_{th} , leading to a degenerate minimum in the minimization procedure of the rate function $J(\eta)$.

-
- [1] U. Seifert, Stochastic thermodynamics, fluctuation theorems and molecular machines, Rep. Prog. Phys. **75**, 126001 (2012).
 - [2] S. J. Blundell and K. M. Blundell, *Concepts in Thermal Physics*, (Oxford University Press, Oxford, 2006).
 - [3] R. S. Ellis, *Entropy, Large Deviations, and Statistical Mechanics*, (Springer, Berlin, 1985).
 - [4] Y. Oono, Large deviation and statistical physics, Prog. Theoret. Phys. Suppl. **99**, 165 (1989).
 - [5] A. Dembo and O. Zeitouni, *Large Deviations Techniques and Applications*, (Springer, Berlin, 1998).
 - [6] H. Touchette, The large deviation approach to statistical mechanics, Phys. Rep. **478**, 1 (2009).
 - [7] G. Verley, M. Esposito, T. Willaert and C. Van den Broeck, The unlikely Carnot efficiency, Nat. Comm. **5**, 4721 (2014).
 - [8] G. Verley, T. Willaert, C. Van den Broeck and M. Esposito, Universal theory of efficiency fluctuations, Phys. Rev. E **90**, 052145 (2014).
 - [9] M. Poletini, G. Verley, and M. Esposito, Efficiency Statistics at All Times: Carnot Limit at Finite Power, Phys. Rev. Lett. **114**, 050601 (2015)
 - [10] K. Proesmans and C. Van den Broeck, Stochastic efficiency: five case studies, New J. Phys. **17**, 065004 (2015).
 - [11] K. Proesmans, C. Driesen, B. Cleuren, and C. Van den Broeck, Efficiency of single-particle engines, Phys. Rev. E **92**, 032105 (2015).
 - [12] M. Esposito, M.A. Ochoa, and M. Galperin, Efficiency fluctuations in quantum thermoelectric devices, Phys. Rev. B **91**, 115417 (2015).
 - [13] G. B. Cuetara and M. Esposito, Double quantum dot coupled to a quantum point contact: a stochastic thermodynamics approach, New J. Phys. **17**, 095005 (2015).
 - [14] J. Jiang, B. K. Agarwalla and D. Segal, Efficiency Statistics and Bounds for Systems with Broken Time-Reversal Symmetry, Phys. Rev. Lett. **115**, 040601 (2015).
 - [15] B. K. Agarwalla, J.-H. Jiang, and D. Segal, Full counting statistics of vibrationally assisted electronic conduction: Transport and fluctuations of thermoelectric efficiency, Phys. Rev. B **92**, 245418 (2015).
 - [16] K. Proesmans, B. Cleuren, and C. Van den Broeck, Stochastic efficiency for effusion as a thermal engine, EPL **109**, 20004 (2015).
 - [17] J.-M. Park, H.-M. Chun, and J. D. Noh, Efficiency at maximum power and efficiency fluctuations in a linear brownian heat-engine model, Phys. Rev. E **94**, 012127 (2016).
 - [18] D. Gupta and S. Sabhapandit, Stochastic efficiency of an isothermal work-to-work converter engine, Phys. Rev. E **96**, 042130 (2017).
 - [19] M. Sune and A. Imparato, Efficiency fluctuations in steady-state machines, J. Phys. A **52**, 045003 (2019).
 - [20] S. K. Manikandan, L. Dabelow, R. Eichhorn and S. Krishnamurthy, Efficiency Fluctuations in Microscopic Machines, Phys. Rev. Lett. **122**, 140601 (2019).

- [21] H. Vroylandt, M. Esposito, and G. Verley, Efficiency Fluctuations of Stochastic Machines Undergoing a Phase Transition, *Phys. Rev. Lett.* **124**, 250603 (2020).
- [22] M. Esposito, U. Harbola and S. Mukamel, Nonequilibrium fluctuations, fluctuation theorems, and counting statistics in quantum systems, *Rev. Mod. Phys.* **81**, 1665 (2009).
- [23] M. Campisi, P. Hänggi, and P. Talkner, Quantum fluctuation relations: Foundations and applications, *Rev. Mod. Phys.* **83** 771 (2011).
- [24] I. A. Martinez, É. Roldán, L. Dinis, D. Petrov, J. M. R. Parrondo, and R. Rica, Brownian Carnot engine, *Nat. Phys.* **12**, 67 (2015).
- [25] R. Kosloff, A Quantum Mechanical Open System as a Model of a Heat Engine, *J. Chem. Phys.* **80**, 1625 (1984).
- [26] E. Geva and R. Kosloff, A Quantum-Mechanical Heat Engine Operating in Finite Time. A Model Consisting of Spin-1/2 Systems as the Working Fluid, *J. Chem. Phys.* **96**, 3054 (1992).
- [27] M. O. Scully, Quantum Afterburner: Improving the Efficiency of an Ideal Heat Engine, *Phys. Rev. Lett.* **88**, 050602 (2002).
- [28] M. O. Scully, M. S. Zubairy, G. S. Agarwal, and H. Walther, *Science* **299**, 862 (2003).
- [29] B. Lin and J. Chen, Performance Analysis of an Irreversible Quantum Heat Engine Working with Harmonic Oscillators, *Phys. Rev. E* **67**, 046105 (2003).
- [30] T. D. Kieu, The Second law, Maxwell's Demon, and Work Derivable from Quantum Heat Engines, *Phys. Rev. Lett.* **93**, 140403 (2004).
- [31] Y. Rezek and R. Kosloff, Irreversible Performance of a Quantum Harmonic Heat Engine, *New J. Phys.* **8**, 83 (2006).
- [32] H. T. Quan, Y. X. Liu, C. P. Sun, and F. Nori, Nori, Quantum thermodynamic cycles and quantum heat engines, *Phys. Rev. E* **76**, 031105 (2007).
- [33] R. Dillenschneider and E. Lutz, Energetics of quantum correlations, *EPL* **88**, 50003 (2009).
- [34] O. Abah, J. Ronagel, G. Jacob, S. Deffner, F. Schmidt-Kaler, K. Singer, and E. Lutz, Single-Ion Heat Engine at Maximum Power, *Phys. Rev. Lett.* **109**, 203006 (2012).
- [35] K. Zhang, F. Bariani, and P. Meystre, Quantum Optomechanical Heat Engine, *Phys. Rev. Lett.* **112**, 150602 (2014).
- [36] G. Watanabe, B. P. Venkatesh, P. Talkner, and A. del Campo, Quantum Performance of Thermal Machines over Many Cycles, *Phys. Rev. Lett.* **118**, 050601 (2017).
- [37] J. Ronagel, S. T. Dawkins, K. N. Tolazzi, O. Abah, E. Lutz, F. Schmidt-Kaler, and K. Singer, A single-atom heat engine, *Science* **352**, 325 (2016).
- [38] J. P. S. Peterson, T. B. Batalhao, M. Herrera, A. M. Souza, R. S. Sarthour, I. S. Oliveira, and R. M. Serra, Experimental characterization of a spin quantum heat engine, *Phys. Rev. Lett.* **123**, 240601 (2019).
- [39] R. J. de Assis, T. M. de Mendonca, C. J. Villas-Boas, A. M. de Souza, R. S. Sarthour, I. S. Oliveira, and N. G. de Almeida, Efficiency of a Quantum Otto Heat Engine Operating under a Reservoir at Effective Negative Temperatures, *Phys. Rev. Lett.* **122**, 240602 (2019).
- [40] N. Van Horne, D. Yum, T. Dutta, P. Hänggi, J. Gong, D. Poletti and M. Mukherjee, Single-atom energy-conversion device with a quantum load, *npj Quantum Information* **6**, 37 (2020).
- [41] R. Kosloff and Y. Rezek, The Quantum Harmonic Otto Cycle, *Entropy*, **19**, 136 (2017).
- [42] A. del Campo, J. Goold, and M. Paternostro, More bang for your buck: Super-adiabatic quantum engines, *Sci. Rep.* **4**, 6208 (2014).
- [43] O. Abah and E. Lutz, Energy efficient quantum machines, *EPL* **118**, 40005 (2017).
- [44] O. Abah and E. Lutz, Performance of shortcut-to-adiabaticity quantum engines, *Phys. Rev. E* **98**, 032121 (2018).
- [45] V. Gritsev, P. Barmettler, and E. Demler, Scaling approach to quantum non-equilibrium dynamics of many-body systems, *New J. Phys.* **12**, 113005 (2010).
- [46] C. Jarzynski, Generating shortcuts to adiabaticity in quantum and classical dynamics, *Phys. Rev. A* **88**, 040101(R) (2013).
- [47] A. del Campo, Shortcuts to Adiabaticity by Counterdiabatic Driving, *Phys. Rev. Lett.* **111**, 100502 (2013).
- [48] S. Deffner, C. Jarzynski and A. del Campo, Classical and Quantum Shortcuts to Adiabaticity for Scale-Invariant Driving, *Phys. Rev. X* **4**, 021013 (2014).
- [49] M. Beau, J. Jaramillo and A. del Campo, Scaling-Up Quantum Heat Engines Efficiently via Shortcuts to Adiabaticity, *Entropy* **18**(5), 168 (2016).
- [50] C. Jarzynski, H. T. Quan, and S. Rahav, Quantum-Classical Correspondence Principle for Work Distributions, *Phys. Rev. X* **5**, 031038 (2015).
- [51] A. Papoulis, *Probability, Random Variables and Stochastic Processes*, (McGraw-Hill, New York, 1991).
- [52] M. Campisi, J. Pekola, and R. Fazio, Nonequilibrium fluctuations in quantum heat engines: Theory, example, and possible solid state experiments, *New J. Phys.* **17**, 035012 (2015).
- [53] P. Talkner, E. Lutz and P. Hänggi, Fluctuation theorems: Work is not an observable, *Phys. Rev. E* **75**, 050102(R). [54] See Supplemental Material.
- [55] R. J. Barlow, *Statistics*, (Wiley, New York, 1989).
- [56] S. Deffner and E. Lutz, Nonequilibrium work distribution of a quantum harmonic oscillator, *Phys. Rev. E* **77**, 021128 (2008).
- [57] S. Deffner, O. Abah, and E. Lutz, Quantum work statistics of linear and nonlinear parametric oscillators, *Chem. Phys.* **375**, 200 (2010).
- [58] M. Esposito, R. Kawai, K. Lindenberg, and C. Van den Broeck, Efficiency at Maximum Power of Low-Dissipation Carnot Engines, *Phys. Rev. Lett.* **105**, 150603 (2010).
- [59] V. Cavina, A. Mari, and V. Giovannetti, Slow Dynamics and Thermodynamics of Open Quantum Systems, *Phys. Rev. Lett.* **119**, 050601 (2017).
- [60] P. Abiuso and M. Perarnau-Llobet, Optimal Cycles for Low-Dissipation Heat Engines, *Phys. Rev. Lett.* **124**, 110606 (2020).
- [61] C. Jarzynski and D. K. Wójcik, Classical and Quantum Fluctuation Theorems for Heat Exchange, *Phys. Rev. Lett.* **92**, 230602 (2004).
- [62] T. Denzler and E. Lutz, Efficiency statistics of a quantum heat engine, *Phys. Rev. Research* (2020), in press.
- [63] E. Barnes and S. Das Sarma, Analytically Solvable Driven Time-Dependent Two-Level Quantum Systems, *Phys. Rev. Lett.* **109**, 060401 (2012).
- [64] E. Barnes, Analytically solvable two-level quantum systems and Landau-Zener interferometry, *Phys. Rev. A* **88**, 013818 (2013).